Transactions of the Materials Research Society of Japan 29[4] 1675-1678 (2004)

Effect of Additives and Ribbon Thickness on Magnetic Properties in Nanocrystalline $Fe_{9.4-x}Co_{70}Nb_{2.6}Si_9B_9M_x$ Alloys (M: Nb, Zr, W, Mo, V, Cr, Ti, Ni, Si, Al, Ga)

Yoshihito Yoshizawa and Shigeo Fujii
Advanced Electronics Research Laboratory, Hitachi Metals, Ltd., Japan
Fax: 81-48-533-7102, e-mail: yoshihito_yoshizawa@hitachi-metals.co.jp

The effects of additives and ribbon thickness on magnetic properties have been studied in Co-rich nanocrystalline FeCoNbSiB alloys annealed under a transverse field. Adding Ni to FeCoNbSiB alloy is effective to increase quality factor, *Q* in the high frequency range. The *Q* increased with decreasing ribbon thickness. The $Fe_{7.4}Co_{70}Nb_{2.6}Si_9B_9Ni_2$ alloy of 10 μm thick showed the high *Q* of 32.4 at 1 MHz.
Key words: nanocrystalline, magnetic properties, FeCoNbSiB, magnetic field annealing

1. INTRODUCTION

Nanocrystalline FeCuNbSiB soft magnetic alloys show attractive magnetic properties such as high magnetic induction, high permeability and low core loss [1-3]. The nanocrystalline microstructure of the FeCuNbSiB alloys is produced by crystallizing the amorphous alloys. The mechanism of the grain refinement for the FeCuNbSiB alloys has been extensively studied by atom-probe field ion microscopy and three-dimensional atom-probe [4, 5]. After our reports, FeZrB and FeCoCuZrB alloys were reported as nanocrystalline materials with high magnetic induction or high Curie temperature [6, 7]. Among these nanocrystalline alloys, the FeCuNbSiB alloys are most widely used in industrial electronics due to their excellent magnetic properties [8]. However, excellent magnetic properties in the higher frequency range are presently required for soft magnetic materials because of the recent increase of operating frequency in electronic equipment. The control of induced magnetic anisotropy and hysteresis loop shape is particularly important for soft magnetic materials used in magnetic components for applications in the high frequency range and high power range. Recently, Yoshizawa *et al.* reported that Co-rich nanocrystalline FeCoCuNbSiB alloys annealed under a transverse magnetic field, show flat B-H loops, high quality factor, Q $(=\mu'/\mu'')$ around 1 MHz and large induced magnetic anisotropy [9]. In addition, it was found that the Co-rich alloy containing about 70 at% Co exhibits the highest *Q* at 1 MHz. Recently, it was also reported that nanocrystalline microstructure and soft magnetic properties do not necessary require adding Cu to the Co-rich FeCoNbSiB alloys [10]. The aim of this study is to improve the magnetic properties of the nanocrystalline Co-rich nanocrystalline FeCoNbSiB alloys in the high frequency range by adding some elements and decreasing ribbon thickness.

2. EXPERIMENTAL PROCEDURE

Amorphous $Fe_{9.4-x}Co_{70}Nb_{2.6}Si_9B_9M_x$ (M: Nb, Zr, W, Mo, V, Cr, Ti, Ni, Si, Al, Ga) alloy ribbons were prepared by the single roller melt spinning technique. The ribbons were 5 mm in width. Typical ribbon thickness was 18 μm. Toroidal core specimens having outer and inner diameters of 19 and 15 mm, respectively, were fabricated by winding the ribbons. These samples were annealed at 803 K for 3.6 ks to induce nanocrystallization under a transverse magnetic field of 240 kA m^{-1} within a nitrogen gas atmosphere. d.c. B-H loops, complex relative permeability (quality factor, *Q*) and core loss were measured with an automatic hysteresis loop tracer, a network analyzer and a B-H analyzer, respectively. The induced magnetic anisotropy was estimated from the anisotropy field H_K determined from the d.c. B-H loops. The constituent phases in these specimens were identified by X-ray diffraction (XRD). The microstructure was observed by transmission electron microscopy (TEM). The electrical resistivity was measured by four-point probe method.

3. RESULTS AND DISCUSSION

3.1 Effect of additives

Fig. 1 shows the dependence of magnetic induction at

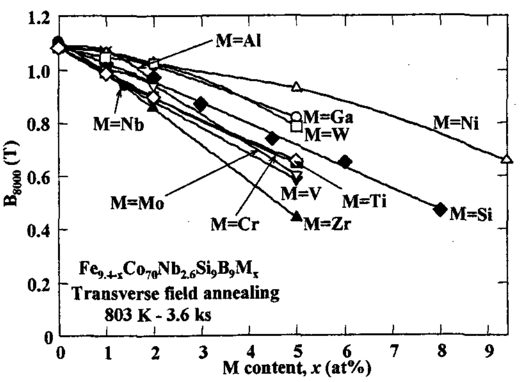

Fig. 1 Dependence of B_{8000} on M content, *x* for $Fe_{9.4-x}Co_{70}Nb_{2.6}Si_9B_9M_x$ alloys (M: Nb, Zr, W, Mo, V, Cr, Ti, Ni, Si, Al, Ga).

8000 A m^{-1}, B_{8000} on M content, x for $Fe_{9.4-x}Co_{70}Nb_{2.6}Si_9B_9M_x$ alloys (M: Nb, Zr, W, Mo, V, Cr, Ti, Ni, Si, Al, Ga) annealed under a transverse magnetic field. The magnetic induction, B_{8000} decreases monotonously with M content, x. The samples M=Ni exhibit relatively a slight decrease of the B_{8000} with M content. On the other hand, the samples M=Nb, Zr show the remarkable decrease of B_{8000} with M content.

Fig. 2 shows the dependence of Q at 1 MHz on M content, x for $Fe_{9.4-x}Co_{70}Nb_{2.6}Si_9B_9M_x$ alloys (M: Nb, Zr, W, Mo, V, Cr, Ti, Ni, Si, Al, Ga) with 18 µm thick annealed under a transverse magnetic field. It was

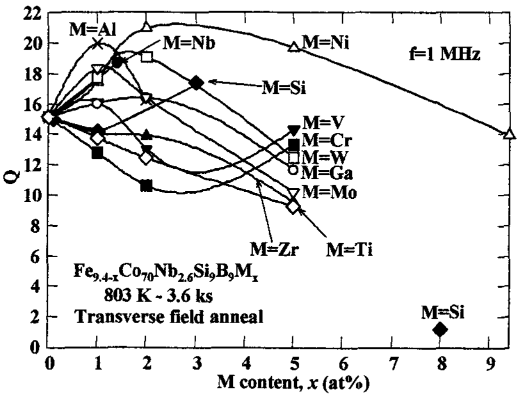

Fig. 2 Dependence of Q at 1 MHz on M content, x for $Fe_{9.4-x}Co_{70}Nb_{2.6}Si_9B_9M_x$ alloys (M: Nb, Zr, W, Mo, V, Cr, Ti, Ni, Si, Al, Ga).

identified that these samples crystallizes except for the alloy of x=8 (M=Si) from XRD analysis. The Q of the alloys adding Nb, W, Mo, Al, Ni, Si and Ga shows the maximum value of the Q at x=1 - 3. In particular, the alloy containing 2 at% Ni shows the highest Q of 21. This Q value is about 39 times higher than that of a Co-free $Fe_{78.8}Cu_{0.6}Nb_{2.6}Si_9B_9$ alloy [9]. Thus, adding small amount of Ni is effective for increasing the Q. On the other hand, in the samples M=Zr, Ti and Cr, the Q decreases monotonously with M content.

Fig. 3 shows the dependence of induced magnetic anisotropy constant K_u on M content, x for $Fe_{9.4-x}Co_{70}Nb_{2.6}Si_9B_9M_x$ alloys (M: Nb, Zr, W, Mo, V, Cr, Ti, Ni, Si, Al, Ga) annealed under a magnetic field.

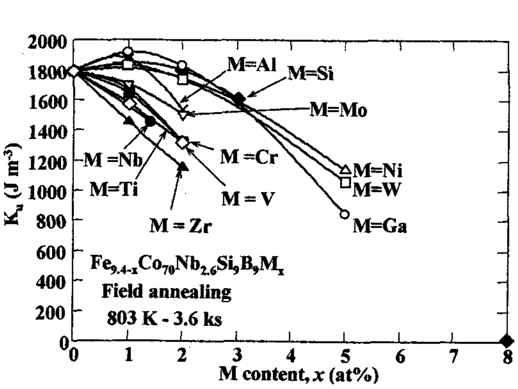

Fig. 3 Dependence of induced magnetic anisotropy constant K_u on M content, x for $Fe_{9.4-x}Co_{70}Nb_{2.6}Si_9B_9M_x$ alloys (M: Nb, Zr, W, Mo, V, Cr, Ti, Ni, Si, Al, Ga).

The K_u for the samples M=Ga, Al, W, Ni and Si shows the maximum values at x=1. On the other hand, the K_u for the samples M=Mo, Cr, V, Nb, Ti and Zr decreases monotonously with M content. The elements of increasing the K_u are approximately the same as the elements of increasing the Q at 1MHz. Hence, the increase of the K_u appears to contribute considerably to the increase of the Q.

Fig.4 shows the dependence of electrical resistivity on M content, x for the samples M=Nb, Zr, W, Mo, V, Cr, Ti, Ni, Si, Al and Ga. The electrical resistivity of the samples increases with M content, x except the sample with 5 at% Ga. Therefore, the decrease of eddy current as well as the increase of the K_u with M content appears to contribute to the increase of the Q for most of the samples.

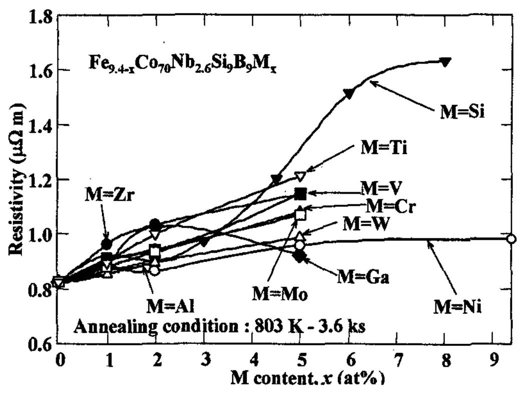

Fig. 4 Dependence of electrical resistivity on M content, x for $Fe_{9.4-x}Co_{70}Nb_{2.6}Si_9B_9M_x$ alloys (M: Nb, Zr, W, Mo, V, Cr, Ti, Ni, Si, Al, Ga).

Fig. 5 shows XRD profiles of as-quenched and annealed $Fe_{7.4}Co_{70}Nb_{2.6}Si_9B_9Ni_x$ alloys (x=0, 2). The XRD profile of the as-quenched $Fe_{7.4}Co_{70}Nb_{2.6}Si_9B_9Ni_x$ alloys (x=0, 2) shows halo pattern typical to amorphous alloys. However, a small peak corresponding to an fcc phase exists on the hallo pattern. Hence, the as-quenched samples consist of an amorphous phase and a little fcc phase. The XRD profiles of the annealed $Fe_{7.4}Co_{70}Nb_{2.6}Si_9B_9Ni_x$ alloys (x=0, 2) show main phase peaks from bcc phase and the small peak from fcc phase. This shows that the bcc phase is formed in annealing

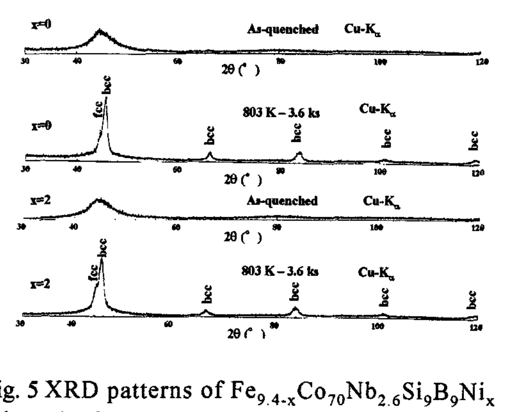

Fig. 5 XRD patterns of $Fe_{9.4-x}Co_{70}Nb_{2.6}Si_9B_9Ni_x$ alloys (x=0, 2).

process and the fcc phase is mainly formed in rapid quenching process.

Fig. 6 shows the TEM bright field micrograph of the $Fe_{7.4}Co_{70}Nb_{2.6}Si_9B_9Ni_2$ alloy annealed at 803 K for 3.6 ks. The nano-scale grains with average grain size of about 8 nm are observed in the $Fe_{7.4}Co_{70}Nb_{2.6}Si_9B_9Ni_2$ alloy. From the XRD results, it is concluded that these grains consist mainly of a bcc phase and the bcc grains seem to play a role in high Q and high K_u.

3.2 Effect of ribbon thickness

It is well known that the eddy current loss can decrease by decreasing ribbon thickness. Therefore, the thickness dependence was studied to improve the properties in the high frequency range.

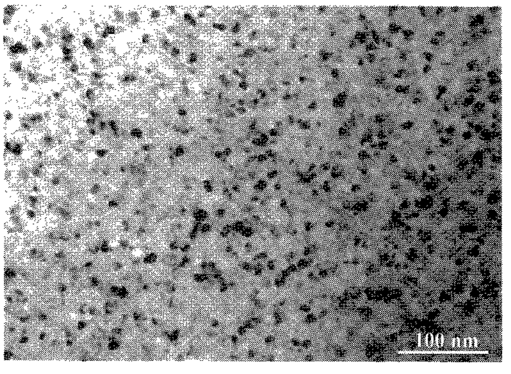

Fig. 6 TEM bright field micrograph of the $Fe_{7.4}Co_{70}Nb_{2.6}Si_9B_9Ni_2$ alloy annealed at 803 K for 3.6 ks.

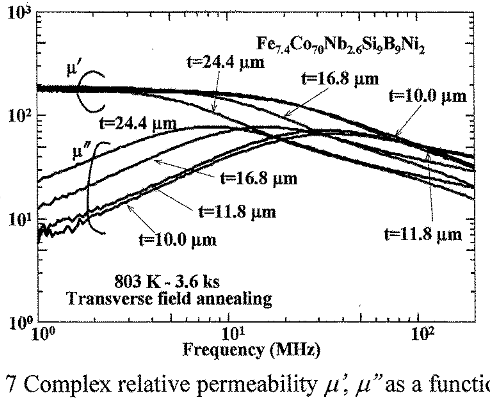

Fig. 7 Complex relative permeability μ', μ'' as a function of frequency for nanocrystalline $Fe_{7.4}Co_{70}Nb_{2.6}Si_9B_9Ni_2$ alloys with different ribbon thickness.

Fig. 7 shows the complex relative permeability μ', μ'' as a function of frequency for nanocrystalline $Fe_{7.4}Co_{70}Nb_{2.6}Si_9B_9Ni_2$ alloys with different ribbon thickness annealed under a transverse magnetic field. The thinner samples show the constant μ' of about 200 up to higher frequency. In particular, the μ' of the sample with 10 μm in thickness keep almost constant value up to about 10 MHz. The frequency, where the maximum value of the μ'' is obtained, shifts to higher frequency with decreasing ribbon thickness. As a result, the frequency, where the maximum of the μ'' is obtained, is beyond 10 MHz. As shown in this figure, the dependence of permeability on frequency is improved.

Fig. 8 shows the dependence of Q at 1 MHz for nanocrystalline $Fe_{7.4}Co_{70}Nb_{2.6}Si_9B_9Ni_2$ alloys annealed under a transverse magnetic field. The Q at 1 MHz

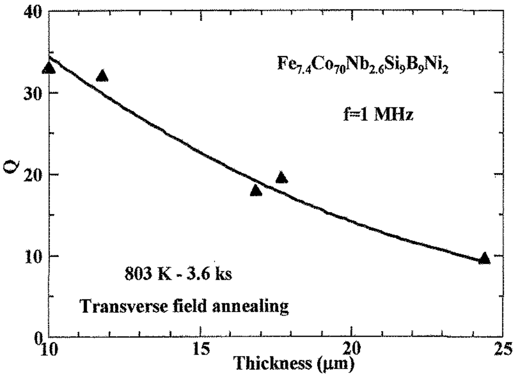

Fig. 8 Dependence of Q at 1 MHz for nanocrystalline $Fe_{7.4}Co_{70}Nb_{2.6}Si_9B_9Ni_2$ alloys.

increases with decreasing ribbon thickness. The high Q of 32.4 was obtained at 10 μm thick. The Q value is about 1.5 times higher than that of the alloy with the same composition and with 18 μm thick. Thus, the Q at 1 MHz of the nanocrystalline $Fe_{7.4}Co_{70}Nb_{2.6}Si_9B_9Ni_2$ alloy is remarkably improved with decreasing ribbon thickness. The high Q of the nanocrystalline $Fe_{7.4}Co_{70}Nb_{2.6}Si_9B_9Ni_2$ alloy with 10 μm in thickness results from the decrease of eddy current loss due to the decrease of the ribbon thickness. In addition, we found that nanocrystalline $Fe_{6.8}Co_{70}Cu_{0.6}Nb_{2.6}Si_9B_9Ni_2$ alloys adding Cu show similar good properties in the high frequency range. The highest Q at 1 MHz of 34.3 was obtained in the nanocrystalline Co-rich $Fe_{6.8}Co_{70}Cu_{0.6}Nb_{2.6}Si_9B_9Ni_2$ alloy with 11 μm thick. Thus, the decrease of ribbon thickness improves the Q of the nanocrystalline Co-rich alloys in the high frequency range.

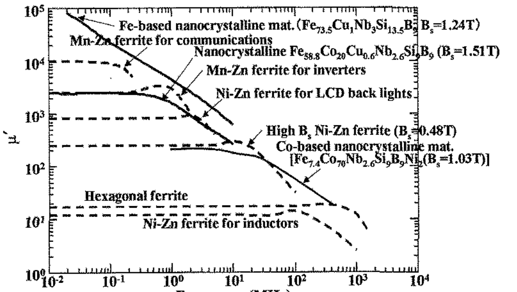

Fig. 9 Dependence of μ' on frequency for various nanocrystalline soft magnetic materials and soft ferrites.

Fig. 9 shows the dependence of μ' on frequency for various nanocrystalline soft magnetic materials and soft ferrites. The μ' of the nanocrystalline Fe-based alloy begins to decrease from frequency beyond about 10 kHz. On the other hand, the dependence of the μ' on frequency for the nanocrystalline Co-rich $Fe_{7.4}Co_{70}Nb_{2.6}Si_9B_9$ alloy (B_s=1.03 T) is approximately comparable to that for the soft ferrite (B_s=0.48 T) with

Table I Magnetic properties and electrical properties of nanocrystalline alloys with flat B-H loops.

Composition (at %)	t (μm)	B_{8000} (T)	$B_r B_{8000}^{-1}$ (%)	H_c (A m^{-1})	μ′	P_{cv} (kW m^{-3})	Q	K_u (J m^{-3})	ρ (μΩ m)
$Fe_{7.4}Co_{70}Nb_{2.6}Si_9B_9Ni_2$	10	1.03	2	55.7	180	—	32.4	1700	0.86
$Fe_{7.4}Co_{70}Nb_{2.6}Si_9B_9Ni_2$	18	1.03	1	44.6	190	480	21.0	1750	0.86
$Fe_{6.8}Co_{70}Cu_{0.6}Nb_{2.6}Si_9B_9Ni_2$	11	1.01	3	51.2	180	—	34.3	1680	0.88
$Fe_{6.8}Co_{70}Nb_{2.6}Si_{11}B_9$	18	0.97	2	69.0	140	—	24.2	1800	0.92
$Fe_{8.8}Co_{70}Cu_{0.6}Nb_{2.6}Si_9B_9$	18	1.08	1	30.3	205	620	13.9	1840	0.83
$Fe_{9.4}Co_{70}Nb_{2.6}Si_9B_9$	18	1.11	1	36.7	200	400	14.9	1790	0.84
$Fe_{78.8}Cu_{0.6}Nb_{2.6}Si_9B_9$	18	1.53	3	2.6	7800	280	0.54	96	1.13
$Fe_{73.5}Cu_1Nb_3Si_{13.5}B_9$	18	1.24	11	0.8	22000	230	0.68	15	1.2

B_{8000} : Magnetic induction at 8000 A m^{-1} μ′ : Relative permeability (real part) at 100 kHz, 0.05A m^{-1}
P_{cv} : Core loss per core volume at 100 kHz, 0.2 T Q: Quality factor at 1 MHz

about half B_s of the nanocrystalline Co-rich $Fe_{7.4}Co_{70}Nb_{2.6}Si_9B_9Ni_2$ alloy. Hence, the nanocrystalline Co-based alloys are suitable for power electronics applications in the high frequency range due to their high magnetic induction and good magnetic properties in the high frequency range. The use of the Co-rich nanocrystalline alloys can make it possible to miniaturize magnetic parts such as power inductors for applications in the high frequency range.

Table I summarizes the magnetic properties and the electrical properties of nanocrystalline alloys with flat B-H loops. The alloys found in this work exhibit the B_s of about 1 T, high Q beyond 20 and high K_u. In addition, these alloys show low core loss as compared with the materials showing low μ' of from 100 to 300 and a flat B-H loop. Hence, the Co-rich nanocrystalline alloys are promising for power electronics applications such as power inductors in the high frequency range, because of their high B_s, flat B-H loop, and low loss.

4. CONCLUSIONS

We have investigated the effects of additives and ribbon thickness on magnetic properties in Co-rich nanocrystalline FeCoNbSiB alloys annealed under a transverse field to improve the high frequency soft magnetic properties, and following conclusions were obtained.

(1) The Q at 1 MHz of the $Fe_{9.4-x}Co_{70}Nb_{2.6}Si_9B_9M_x$ alloys (M: Nb, W, Mo, Al, Ni, Si, and Ga) shows the maximum value at x=1 – 3.

(2) The maximum Q of 34.3 at 1 MHz was obtained in the nanocrystalline $Fe_{16.8}Co_{70}Cu_{0.6}Nb_{2.6}Si_9B_9Ni_2$ alloy with 11 μm thick.

(3) The increase of K_u, the increase of electrical resistivity and the decrease of ribbon thickness are effective for increasing Q of the nanocrystalline Co-rich alloys in the high frequency range.

(4) The Co-rich nanocrystalline alloys are promising for high frequency applications such as power inductors due to their high B_s, flat B-H loop, high Q, and low core loss.

Acknowledgment

This work was partly supported by the Special Coordination Funds for Promoting Science and Technology on "Nanohetero Metallic Materials" from the Ministry of Education, Sports, Culture, Science and Technology of Japan.

References

[1] Y. Yoshizawa, S. Oguma and K. Yamauchi, *J. Appl. Phys.*, **64**, 6044-46 (1988).
[2] Y. Yoshizawa, K. Yamauchi, *Mater. Trans., JIM*, **31**, 307-14 (1990).
[3] Y. Yoshizawa, *Scripta mater.*, **44**, 1321-25(2001).
[4] K. Hono, K. Hiraga, Q. Wang, A. Inoue, T. Sakurai, *Acta Metall.*, **40**, 2137-2147(1992).
[5] K. Hono, D. H. Ping, M. Ohnuma, H. Onodera, *Acta Mater.*, **47**, 997-06 (1999).
[6] K. Suzuki, N. Kataoka, A. Inoue, A. Makino and T. Masumoto, *Mater. Trans., JIM*, **31**, 743-46 (1990).
[7] M. A. Willard, D. F. Laughlin, M. E. McHenry, D. Thomas, K. Sickafus, J. O. Cross and V. G. Harris, *J. Appl. Phys.*, **84**, 6773-77(1998).
[8] Y. Yoshizawa, *Mater. Sci. Forum*, **307**, 51-62(1999).
[9] Y. Yoshizawa, S. Fujii, D. H. Ping, M. Ohnuma and K. Hono, *Scr. Mater.*, **48**, 863-68(2003).
[10] Y. Yoshizawa, S. Fujii, D. H. Ping, M. Ohnuma and K. Hono, *Mater. Sci. Eng. A*. in press.

(Received October 8, 2003; Accepted February 9, 2004)